

## Accepted Manuscript

A coumarin-derived Cu<sup>2+</sup>-fluorescent chemosensor and its direct application in aqueous media

Naveen Mergu, Myeongjin Kim, Young-A. Son



PII: S1386-1425(17)30607-8

DOI: doi: [10.1016/j.saa.2017.07.047](https://doi.org/10.1016/j.saa.2017.07.047)

Reference: SAA 15334

To appear in: *Spectrochimica Acta Part A: Molecular and Biomolecular Spectroscopy*

Received date: 22 May 2017

Revised date: 12 July 2017

Accepted date: 24 July 2017

Please cite this article as: Naveen Mergu, Myeongjin Kim, Young-A. Son , A coumarin-derived Cu<sup>2+</sup>-fluorescent chemosensor and its direct application in aqueous media, *Spectrochimica Acta Part A: Molecular and Biomolecular Spectroscopy* (2017), doi: [10.1016/j.saa.2017.07.047](https://doi.org/10.1016/j.saa.2017.07.047)

This is a PDF file of an unedited manuscript that has been accepted for publication. As a service to our customers we are providing this early version of the manuscript. The manuscript will undergo copyediting, typesetting, and review of the resulting proof before it is published in its final form. Please note that during the production process errors may be discovered which could affect the content, and all legal disclaimers that apply to the journal pertain.

**A coumarin-derived Cu<sup>2+</sup>-fluorescent chemosensor and its direct application  
in aqueous media**

Naveen Mergu<sup>1</sup>, Myeongjin Kim<sup>1</sup>, Young-A. Son\*

Department of Advanced Organic Materials Engineering, Chungnam National University, 220  
Gung-dong, Yuseong-gu, Daejeon 305-764, South Korea

\*Corresponding author. Tel.: +82 42 821 6620; Fax: +82 42 821 8870.

E-mail addresses: yason@cnu.ac.kr (Y.-A. Son).

<sup>1</sup>These authors contributed equally to this work.

## Abstract

A novel coumarin-based receptor bearing a benzohydrazide (**FCBH**) was developed as a fluorescent chemosensor with high selectivity toward  $\text{Cu}^{2+}$ . The sensor was successfully applied to the monitoring of  $\text{Cu}^{2+}$  in aqueous solution. After the addition of  $\text{Cu}^{2+}$  to **FCBH**, the color of the solution changed from greenish-yellow to red, and the absorption band at 457 nm red-shifted to 517 nm. The fluorescent green color of **FCBH** disappeared and the fluorescence emission was completely quenched in the presence of  $\text{Cu}^{2+}$ . Upon the addition of  $\text{Cu}^{2+}$ , deprotonation of **FCBH** occurred, and a 1:1 metal-ligand complex formed. DFT theoretical investigation was carried out to understand the behavior of the sensing probe toward  $\text{Cu}^{2+}$ . Additionally, the quenched fluorescence of the **FCBH**- $\text{Cu}^{2+}$  complex was restored upon the addition of  $\text{CN}^-$  ions. The possible sensing mechanism of **FCBH** toward  $\text{Cu}^{2+}$  was derived from experimental and theoretical examinations.

**Keywords:** Coumarin, Fluorescence, Chemosensor, Copper, Cyanide, Aqueous media

## 1. Introduction

In the past few years, the development of fluorescent chemosensors for ion and molecular recognition has received increased attention due to their potential applications in biology, medicinal, clinical, catalysis and environmental monitoring [1-5]. Of the many types of techniques, fluorescence sensing has several advantages over other methods such as atomic absorption spectroscopy [6], inductively coupled plasma spectroscopy [7,8], neutron activation analysis [9], chromatography [10], voltammetry [11] and others [12-16] as it possesses intrinsic sensitivity and selectivity, low-cost, convenience, and real-time monitoring with fast response

times [17-20]. The recognition of transition and heavy metal ions, notably of  $\text{Cu}^{2+}$ , is particularly attractive to current researchers, as it is an essential nutrient for life, and both its deficiency and excesses are associated with various disorders [21–23].

Copper is the third most abundant metal among the essential heavy metal ions in the human body [24] and it is crucial in a variety of fundamental physiological processes in organisms [25]. Additionally, it is an essential trace element in biological systems, and its importance may be attributed to its redox nature [26]. Extreme ingestion of copper is harmful due to its ability to generate reactive oxygen species, and it can interfere in cellular metabolism [27]. In addition, unregulated copper can cause various neurodegenerative disorders, including Wilson's disease [28], Alzheimer's disease [29], Parkinson's disease [30] and Menkes disease [31]. According to the US Environmental Protection Agency, the limit of tolerable concentration of  $\text{Cu}^{2+}$  ions in drinking water is  $20 \mu\text{M}$ . Therefore, the detection of copper has been raised as an important consideration. However, while many fluorescent sensing systems for  $\text{Cu}^{2+}$ -selective detection have been reported [32-36], some of them have exhibited low sensitivity, poor selectivity and low water solubility. Therefore, the development of a highly sensitive and selective fluorescent probe for the detection of copper ions with a fast response time in aqueous solution is necessary.

Coumarin derivatives are widely utilized as signaling units in chemosensors due to their excellent chromogenic and fluorogenic properties [37-40]. In our recent study, a 3-formylcoumarin benzoylhydrazone (**FCBH**)-derived fluorescent probe was synthesized and characterized, and its metal ion-recognition properties were investigated for the first time. The **FCBH** probe exhibited highly selective colorimetric and fluorescence quenching recognition of

$\text{Cu}^{2+}$ . Electrospun nanofiber test strips were prepared for the detection of copper ions in aqueous-alcoholic media.

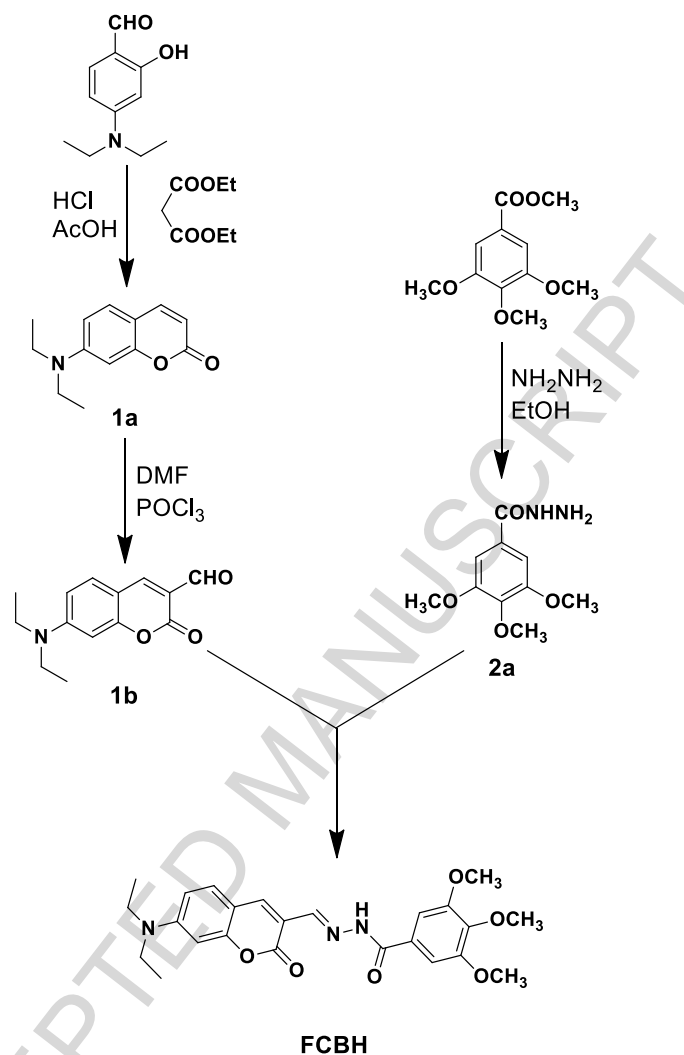
## 2. Experimental

### 2.1. Reagents and apparatus

All the reagents for the synthesis of the **FCBH** chemosensor and metal salts (nitrates and acetates) for the analysis were obtained commercially and used as received. FT-IR spectra were recorded on an ALPHA-P spectrometer.  $^1\text{H}$  and  $^{13}\text{C}$  NMR spectra were performed on a Bruker at 300 and 600 MHz using TMS as an internal standard,  $\text{CDCl}_3$  and  $\text{DMSO-}d_6$  as the solvents. The mass spectra were obtained on a Bruker-microTOF QII mass spectrometer. The UV-Vis absorption spectra and the fluorescence emission spectra were recorded using an Agilent 8453 spectrophotometer and RF-5301PC spectrofluorophotometer, respectively. The excitation and emission slit widths were 3.0 and 1.5 nm, respectively, for the emission studies. DFT calculations were carried out using the Gaussian 09 program at the B3LYP level using the 6-31G\*\* basis set [41]. The geometry optimization was carried out using the M06 [42] hybrid meta exchange correlation density functional at the 6-31G (d,p) level of theory. We performed a population analysis to achieve electron density distribution isosurfaces. SEM images of nanofibers were obtained on a TESCAN-Vega II/LSU. Fluorescence imaging was performed with the Zeiss LSM 5 Live confocal microscope system.

### 2.2. Synthesis and characterization

A coumarin-derived receptor (**FCBH**) was designed and synthesized following the route outlined in Scheme 1.



**Scheme 1.** Synthesis of (E)-N'-((7-(diethylamino)-2-oxo-2H-chromen-3-yl)methylene)-3,4,5-trimethoxybenzohydrazide (**FCBH**).

Compound **1a** was prepared according to the literature method [43]

**7-(Diethylamino)-2-oxo-2H-chromene-3-carbaldehyde (1b):** Anhydrous DMF (2 mL) was added dropwise to POCl<sub>3</sub> (2 mL) at 0 °C and stirred for 30 min to form a white solid. Then, this was combined with a solution of **1a** (1.08 g, 5 mmol) in DMF (10 mL) to create a scarlet suspension. The mixture was stirred at 70 °C for 16 h. After cooling to room temperature, the

mixture was poured into 100 mL of ice water. Upon addition of NaOH (40%) solution to adjust the pH to 5, a large amount of precipitate appeared. The product was filtered, thoroughly washed with water, dried and the residue was purified by column chromatography using DCM/Hexane (90:10) to give the desired compound **1b** as an orange powder (0.75 g, 61%). **1b**: FT-IR (KBr),  $\nu$  ( $\text{cm}^{-1}$ ): 1129, 1256, 1349, 1503, 1569, 1712, 2970;  $^1\text{H}$  NMR ( $\text{CDCl}_3$ , 600 MHz),  $\delta$  (ppm): 1.25 (6H, t,  $J = 7.2$  Hz), 3.47 (4H, q,  $J = 7.2$  Hz), 6.48 (1H, d,  $J = 2.4$  Hz), 6.63 (1H, dd,  $J = 9.0, 2.4$  Hz), 7.40 (1H, d,  $J = 9.0$  Hz), 8.24 (1H, s), 10.12 (1H, s);  $^{13}\text{C}$  NMR ( $\text{CDCl}_3$ , 600 MHz),  $\delta$  (ppm): 12.42, 45.25, 97.14, 108.21, 110.16, 114.31, 132.47, 145.33, 153.44, 158.91, 161.84, 187.90. ESI-MS  $m/z$ : Calcd for  $\text{C}_{14}\text{H}_{15}\text{NO}_3$  ( $\text{M}+\text{Na}$ ) $^+$ : 268.0950, found: 268.0971.

**3,4,5-Trimethoxybenzohydrazide (2a)**: A mixture of methyl 3,4,5-trimethoxybenzoate (0.45 g, 2 mmol) and hydrazine hydrate (55%, 0.64 g, 20 mmol) in 20 mL of ethanol was refluxed for 12 h. After completion of the reaction, the EtOH was evaporated under reduced pressure. Hexane was added into the crude mixture, and the obtained precipitate was filtered and washed with hexane to afford **2a** as a white solid (0.4 g, 89%). **2a**: FT-IR (KBr),  $\nu$  ( $\text{cm}^{-1}$ ): 1126, 1230, 1341, 1581, 3334;  $^1\text{H}$  NMR ( $\text{CDCl}_3$ , 600 MHz),  $\delta$  (ppm): 3.87 (3H, s), 3.88 (6H, s), 6.98 (2H, s), 7.54 (1H, s);  $^{13}\text{C}$  NMR ( $\text{CDCl}_3$ , 600 MHz),  $\delta$  (ppm): 56.3, 60.9, 104.3, 153.3. ESI-MS  $m/z$ : Calcd for  $\text{C}_{10}\text{H}_{14}\text{N}_2\text{O}_4$  ( $\text{M}+\text{Na}$ ) $^+$ : 249.0851, found: 249.0859.

**(E)-N'-((7-(diethylamino)-2-oxo-2H-chromen-3-yl)methylene)-3,4,5-**

**trimethoxybenzohydrazide (FCBH)**: To a solution of 7-diethylamino-3-formylcoumarin (**1b**, 245 mg, 1 mmol) in ethanol (20 mL), 3,4,5-trimethoxybenzohydrazide (**2a**, 226 mg, 1 mmol) was added. The resulting solution was refluxed for 6 h. Then, the solvent was removed and the residue was purified by column chromatography using DCM/MeOH (95:5) to obtain compound **FCBH** as an orange powder (360 mg, 79%). **FCBH**: FT-IR (KBr),  $\nu$  ( $\text{cm}^{-1}$ ): 1072, 1121, 1185,

1226, 1328, 1413, 1501, 1574, 1710, 2969;  $^1\text{H}$  NMR ( $\text{CDCl}_3$ , 600 MHz),  $\delta$  (ppm): 1.22 (6H, t,  $J = 7.2$  Hz), 3.43 (4H, q,  $J = 7.2$  Hz), 3.88 (3H, s), 3.92 (6H, s), 6.43 (1H, s), 6.60 (1H, dd,  $J = 9.0$ , 2.4 Hz), 7.32–7.35 (3H, m), 8.45 (1H, s), 9.67 (1H, s), 10.75 (1H, s);  $^{13}\text{C}$  NMR ( $\text{CDCl}_3$ , 600 MHz),  $\delta$  (ppm): 12.4, 45.0, 56.3, 60.8, 96.9, 105.3, 108.8, 109.8, 112.5, 130.6, 141.2, 151.7, 153.1, 156.8. ESI-MS  $m/z$ : Calcd for  $\text{C}_{24}\text{H}_{27}\text{N}_3\text{O}_6$  ( $\text{M}+\text{Na}$ ) $^+$ : 476.1798, found: 476.1813.

### 2.3. Preparation of electrospun nanofiber (ES) films

The electrospun nanofibers were prepared as presented in our previous report [44]. Briefly, a mixture of dimethylacetamide (DMAc) (60 g), acetone (40 ml) and polyurethane (20 g) was stirred for 12 h at room temperature. After the further slow addition of **FCBH** (45 mg) to this mixture at room temperature, the resulting mixture was stirred for 12 h for fabrication. The resulting clear, homogenous solution was used for electrospinning the film. The blended solution was injected into a metallic needle using syringe pumps (KD Scientific model 200, USA) at a constant rate of 0.5 mL/h. The tip of the metallic needle was connected to a high-voltage power supply (Chungpa EMT, CPS-40K03VIT, Korea) that was set at 15 kV during the ES process. The ES nanofibers were collected on a sheet of aluminum foil.

## 3. Results and discussion

The chemosensor behavior towards various metal ions ( $\text{Zn}^{2+}$ ,  $\text{Pb}^{2+}$ ,  $\text{Al}^{3+}$ ,  $\text{Co}^{2+}$ ,  $\text{Cr}^{3+}$ ,  $\text{Cu}^{2+}$ ,  $\text{Fe}^{3+}$ ,  $\text{Hg}^{2+}$ ,  $\text{Mg}^{2+}$ ,  $\text{Mn}^{2+}$  and  $\text{Ni}^{2+}$ ) was investigated by mass spectrometry and UV-Vis, fluorescence, and proton NMR spectroscopic measurements. Visual detection, absorbance and emission studies were performed in DMSO/water (1:1, v/v) at room temperature.

### 3.1. Colorimetric recognition of $\text{Cu}^{2+}$

The binding ability of **FCBH** to various metal ions was studied by visual examination of the metal-induced color changes in DMSO/water solution. Upon the respective addition of equimolar quantities of  $\text{Zn}^{2+}$ ,  $\text{Pb}^{2+}$ ,  $\text{Al}^{3+}$ ,  $\text{Co}^{2+}$ ,  $\text{Cr}^{3+}$ ,  $\text{Cu}^{2+}$ ,  $\text{Fe}^{3+}$ ,  $\text{Hg}^{2+}$ ,  $\text{Mg}^{2+}$ ,  $\text{Mn}^{2+}$  and  $\text{Ni}^{2+}$  to a 20  $\mu\text{M}$  solution of the **FCBH**, it was found that only  $\text{Cu}^{2+}$  induced a rapid color change. The addition of  $\text{Cu}^{2+}$  caused a visible color change from greenish-yellow to red, as well as green fluorescence quenching (Fig. 1). The color change was attributed to metal coordination with the donor atoms (N and O) in **FCBH**. No color change was observed upon the addition of the other chosen common metal ions. This observation suggests that the **FCBH** probe can serve as a naked-eye colorimetric sensor for  $\text{Cu}^{2+}$ .

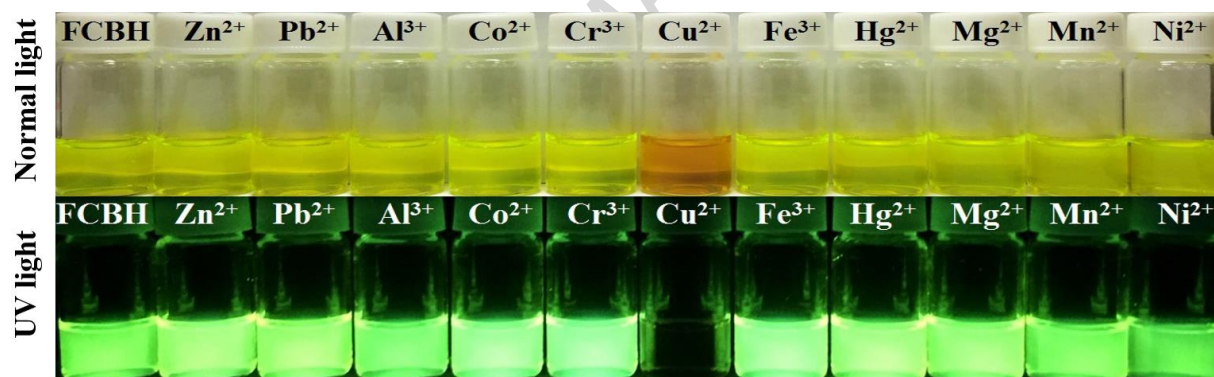


**Fig. 1.** Naked-eye and fluorescence images of **FCBH** (20  $\mu\text{M}$ , DMSO/water, 1:1) upon addition of various metal ions (1 equiv.).

### 3.2. Absorption spectroscopy studies

The UV-Vis spectra for the **FCBH** probe in the presence of various metal ions were recorded in DMSO/water (1:1, v/v). The absorption spectrum of **FCBH** (20  $\mu\text{M}$ ) in DMSO/water (1:1, v/v) showed a major strong band centered at 457 nm (Fig. 2), which corresponds to the n–

$\pi^*$  transition. Upon addition of 1 equiv. of  $\text{Cu}^{2+}$ , the absorption band at 457 nm red-shifted to 517 nm ( $\Delta\lambda = 60$  nm), which was attributed to the intramolecular charge transfer (ICT) transition from the donor to the acceptor [45,46], resulting in a perceived color change from greenish-yellow to red. Other metal ions tested did not induce significant absorption changes under the above conditions. These results indicate that the **FCBH** receptor has a remarkable selectivity to copper ion, which is in good agreement with the colorimetric results.

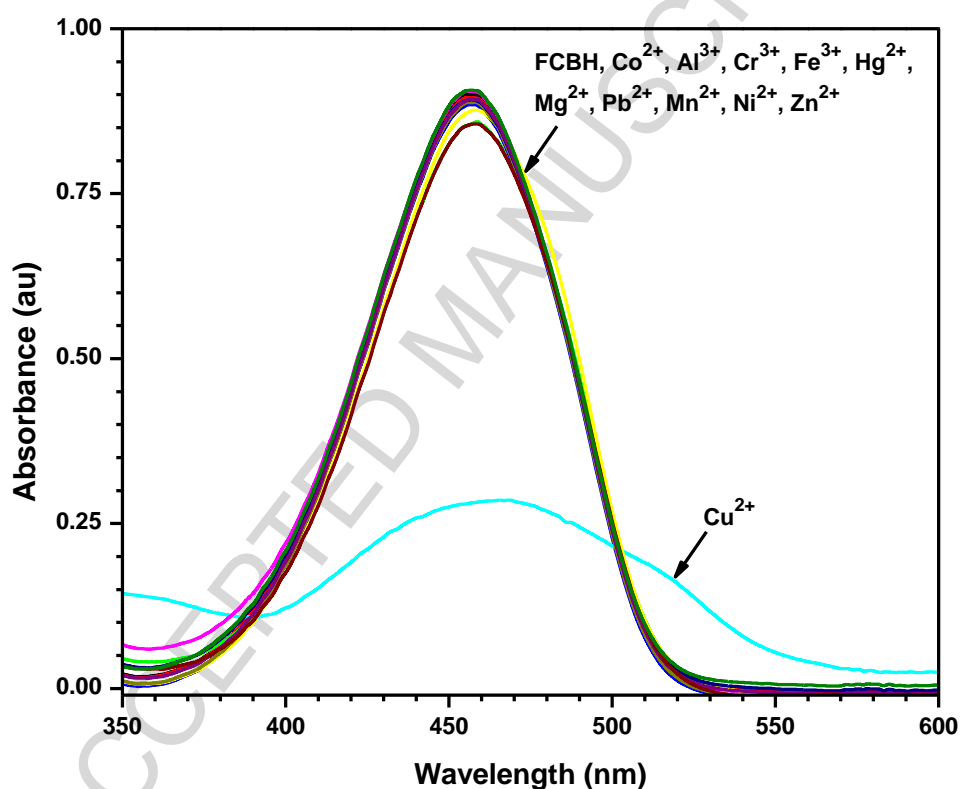


**Fig. 2.** Absorption spectra of **FCBH** (20  $\mu\text{M}$ ) before and after addition of various metal ions (20  $\mu\text{M}$ ).

To elucidate the interactions between **FCBH** and  $\text{Cu}^{2+}$ , UV-Vis titration spectra were recorded with incremental additions (0, 2, 4, 6, 8, 10, 12, 14, 16, 18 and 20  $\mu\text{M}$ ) of  $\text{Cu}^{2+}$ . With

increasing concentration of  $\text{Cu}^{2+}$  (0–1 equiv.), the absorption peak of **FCBH** at 457 nm gradually decreased, and a new peak appeared at 517 nm, no further change was observed above 20  $\mu\text{M}$  (Fig. 3), which may indicate the formation of a new species. This result indicated that the hydrazide was involved in the coordination with  $\text{Cu}^{2+}$ . The changes at 457 and 517 nm were monitored, demonstrating that the absorbance ratios are linearly related to the concentration of  $\text{Cu}^{2+}$  in the 0–20  $\mu\text{M}$  range (Fig. 3, inset), suggesting a 1:1 binding stoichiometry for the M- $\text{Cu}^{2+}$  interactions.

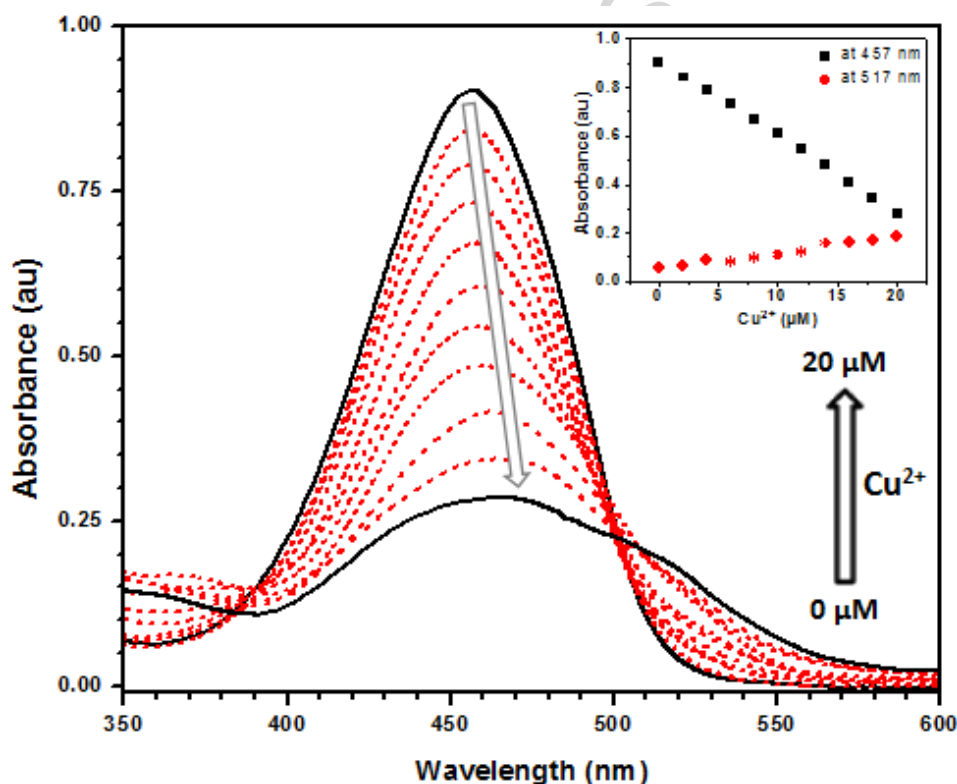


**Fig. 3.** Absorption spectra changes of **FCBH** (20  $\mu\text{M}$ ) after addition of gradual amounts of  $\text{Cu}^{2+}$ . Inset: Absorption at 457 and 517 nm versus the concentration of  $\text{Cu}^{2+}$  added.

### 3.3. Fluorescence emission spectroscopy studies

The fluorescence properties of the **FCBH** receptor were investigated at 450 nm excitation upon the addition of 1 equiv. of  $\text{Zn}^{2+}$ ,  $\text{Pb}^{2+}$ ,  $\text{Al}^{3+}$ ,  $\text{Co}^{2+}$ ,  $\text{Cr}^{3+}$ ,  $\text{Cu}^{2+}$ ,  $\text{Fe}^{3+}$ ,  $\text{Hg}^{2+}$ ,  $\text{Mg}^{2+}$ ,  $\text{Mn}^{2+}$  and  $\text{Ni}^{2+}$  (20  $\mu\text{M}$ ) under the same conditions as mentioned in the absorption study (Fig. 4). The free ligand **FCBH** showed a strong fluorescence emission band at 521 nm with a high quantum yield ( $\Phi = 0.302$ ). Upon addition of  $\text{Cu}^{2+}$ , the fluorescence diminished almost completely, and the fluorescence quantum yield changed to 0.018. This phenomenon could be explained by chelation enhanced fluorescence quenching (CHEQ). Upon addition of  $\text{Cu}^{2+}$  to **FCBH**, a stable chelate complex of  $\text{Cu}^{2+}$  with **FCBH** possibly induces rigidity in the resulting complex, thereby generating efficient chelation-enhanced fluorescence quenching [47]. However, other metal ions did not induce any distinct fluorescence quenching.

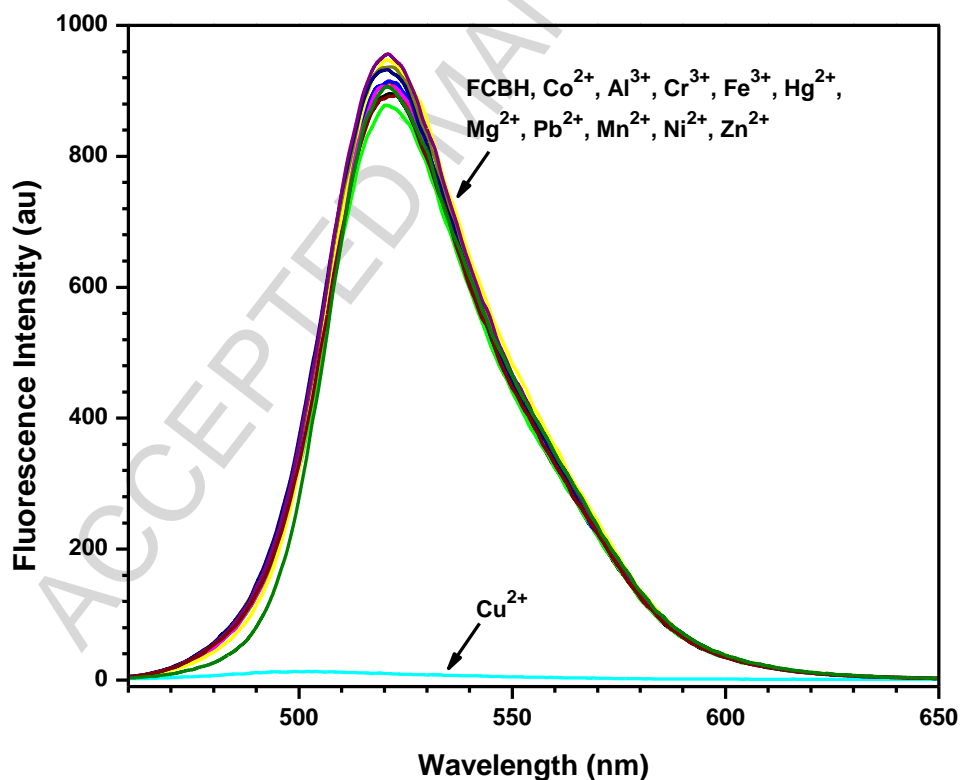


**Fig. 4.** Fluorescence spectra of **FCBH** (20  $\mu\text{M}$ ) before and after addition of various metal ions (20  $\mu\text{M}$ ).

A quantitative investigation of the binding affinity of **FCBH** was also performed by a fluorescence titration experiment with the gradual addition (0, 2, 4, 6, 8, 10, 12, 14, 16, 18 and 20  $\mu\text{M}$ ) of  $\text{Cu}^{2+}$  (Fig. 5). With an increase in the concentration of  $\text{Cu}^{2+}$ , the fluorescence intensity at 521 nm of the probe solution decreased accordingly, and the fluorescence was almost quenched after the addition of 1 equiv. of  $\text{Cu}^{2+}$ . The fluorescence intensity of **FCBH** at 521 nm exhibits a good linear relationship with the concentration of  $\text{Cu}^{2+}$  between 0–20  $\mu\text{M}$  (Fig. 5, inset), which also strongly supports the 1:1 binding stoichiometry of the **FCBH**- $\text{Cu}^{2+}$  complex.

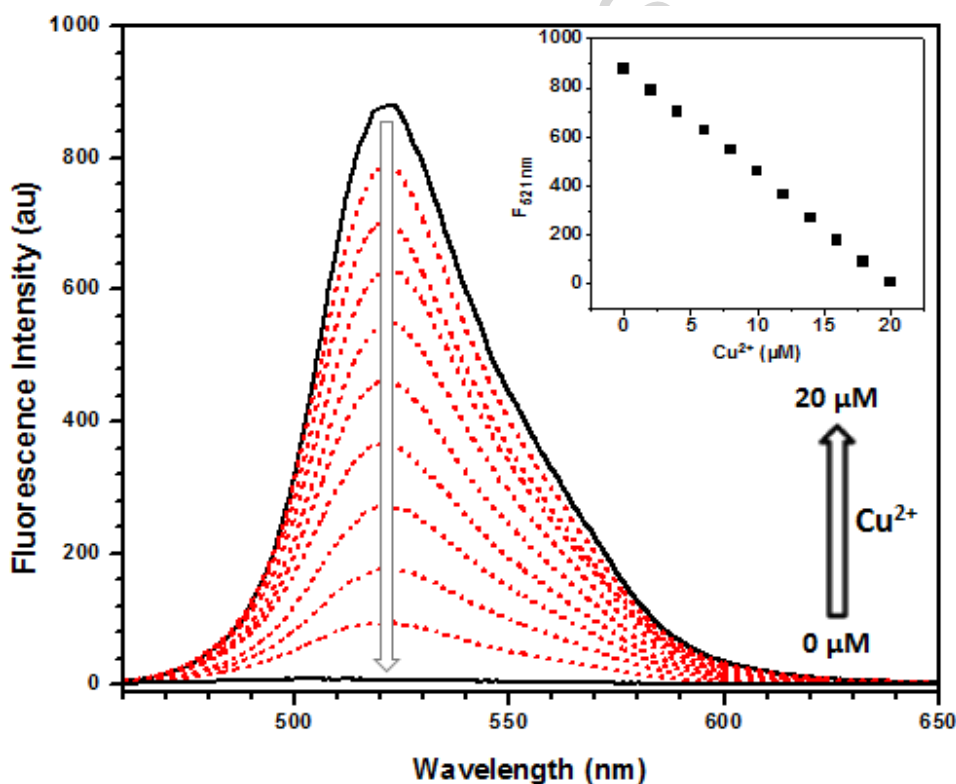


**Fig. 5.** Fluorescence spectra changes of **FCBH** (20  $\mu\text{M}$ ) after addition of the gradual amounts of  $\text{Cu}^{2+}$ . Inset: Fluorescence intensity at 521 nm versus the concentration of  $\text{Cu}^{2+}$  added.

### 3.4. Stoichiometry of the **FCBH**- $\text{Cu}^{2+}$ complex

The stoichiometry of complexation of **FCBH** with  $\text{Cu}^{2+}$  was studied using a Job plot obtained from fluorescence measurements and mass spectrometry analysis. The Job plot revealed that the maximum fluorescence quenching was observed when the mole fraction of  $\text{Cu}^{2+}$  was approximately 0.5, which indicates a 1:1 ligand to metal stoichiometric ratio (Fig. 6). These data were further confirmed by mass analysis. ESI-MS data showed the formation of a 1:1 complex between deprotonated **FCBH** and  $\text{Cu}^{2+}$  (Fig. S1). The observed mass peak at  $m/z$  515.1 corresponded to  $[\text{FCBH} + \text{Cu}^{2+} - \text{H}]^+$  (calcd for  $\text{C}_{24}\text{H}_{26}\text{CuN}_3\text{O}_6$ , 515.1).

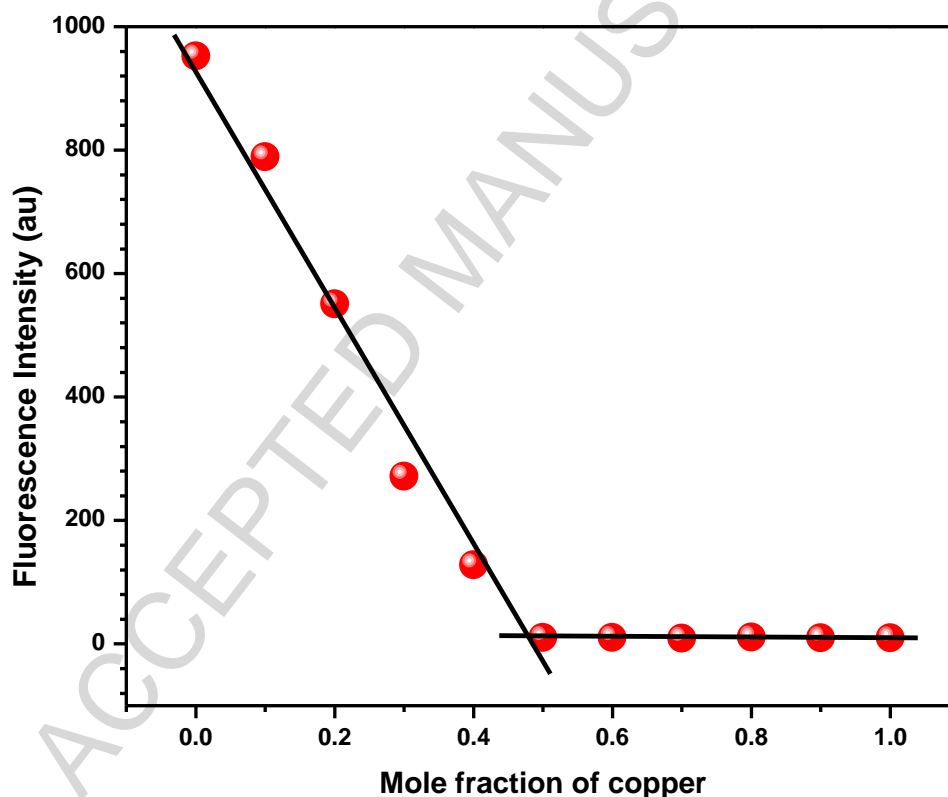


**Fig. 6.** Job plot obtained from fluorescence spectral data, where the intensity of **FCBH** at  $\lambda_{\text{max}}$  of 521 nm was plotted against the mole fraction of  $\text{Cu}^{2+}$ .

### 3.5. $^1\text{H}$ NMR spectroscopy studies

To gain a better understanding the sensing mechanism of **FCBH** towards copper ions, a  $^1\text{H}$  NMR titration experiment was carried out in  $\text{DMSO-}d_6$  at room temperature (Fig. 7).  $\text{Cu}^{2+}$  is a paramagnetic ion that affects the chemical shift ( $\delta$ ) of protons that are close to the  $\text{Cu}^{2+}$  binding site [48]. Upon the addition of  $\text{Cu}^{2+}$  to **FCBH**, almost all the aromatic protons shifted downfield due to the metal ion reducing the electron density on the conjugated receptor system, while no shifts were observed for the aliphatic protons. The most obvious change in chemical shift was noticed for the amide N-H proton. As  $\text{Cu}^{2+}$  ions were added, the N-H proton shifted downfield, and the signal gradually weakened, and then disappeared. The chemical shift signals of the aromatic ring became very broad, weakened and almost completely disappeared upon the addition of  $\text{Cu}^{2+}$ . These observations indicate that  $\text{Cu}^{2+}$  binds to the **FCBH** chemosensor through the N atom of the imine and the O atoms of C=O, which are directly connected to the aromatic rings.

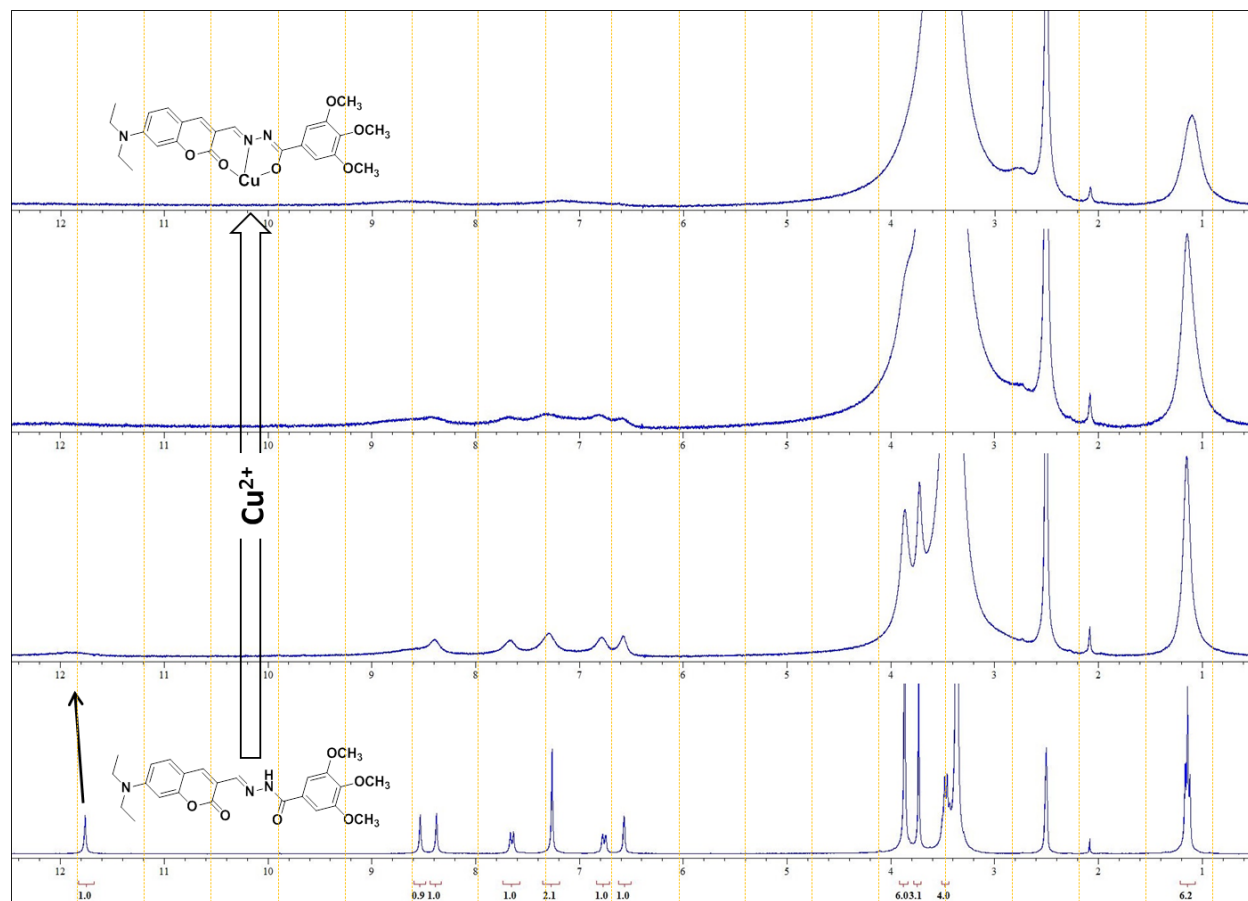
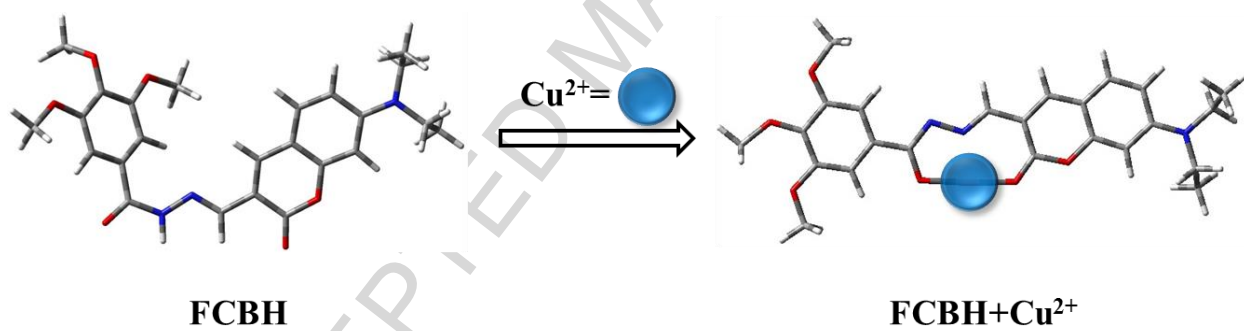


**Fig. 7.**  $^1\text{H}$  NMR (300 MHz) spectral changes of **FCBH** on the addition of  $\text{Cu}(\text{NO}_3)_2$  in  $\text{DMSO-}d_6$ ).

### 3.6. Theoretical (DFT) studies

To better understand their geometry and electronic structure, we carried out DFT calculations for **FCBH** and **FCBH-Cu<sup>2+</sup>**. As shown in Scheme 2, the free receptor was found to adopt a slightly twisted conformation. The geometry converts to planar upon complexation with  $\text{Cu}^{2+}$ . The spatial distributions and orbital energies of the highest occupied molecular orbital (HOMO) and the lowest unoccupied molecular orbital (LUMO) of **FCBH** and **FCBH-Cu<sup>2+</sup>** were also generated using the calculations, as shown in Fig. 8. From the figure, it can be seen that the electron density is mainly delocalized over coumarin hydrazone in the HOMO of **FCBH**, but in

the HOMO of its copper complex, the electron density is located around the metal. The electron density of the LUMO is extended over the whole molecule (mainly coumarin and benzohydrazide) in **FCBH**, whereas in its copper complex it is mainly delocalized over benzohydrazide. The HOMO-LUMO energy gaps of the free receptor and its corresponding copper complex were found to be 3.284 and 2.159 eV, respectively. The decrease in the  $\Delta E$  upon complexation with  $\text{Cu}^{2+}$  corresponds to an ICT transition because the complex of **FCBH**- $\text{Cu}^{2+}$  is a relatively better electron donor than the free receptor. The results demonstrated that the metal complexation of the receptor lowered the HOMO-LUMO energy gap, and the reduction in the energy gap can explain the bathochromic shift in the absorption spectra. Thus, the results obtained from theoretical calculations were in good agreement with the experimental results.



**Scheme 2.** DFT-optimized geometries of **FCBH** and its corresponding  $\text{Cu}^{2+}$  complex.

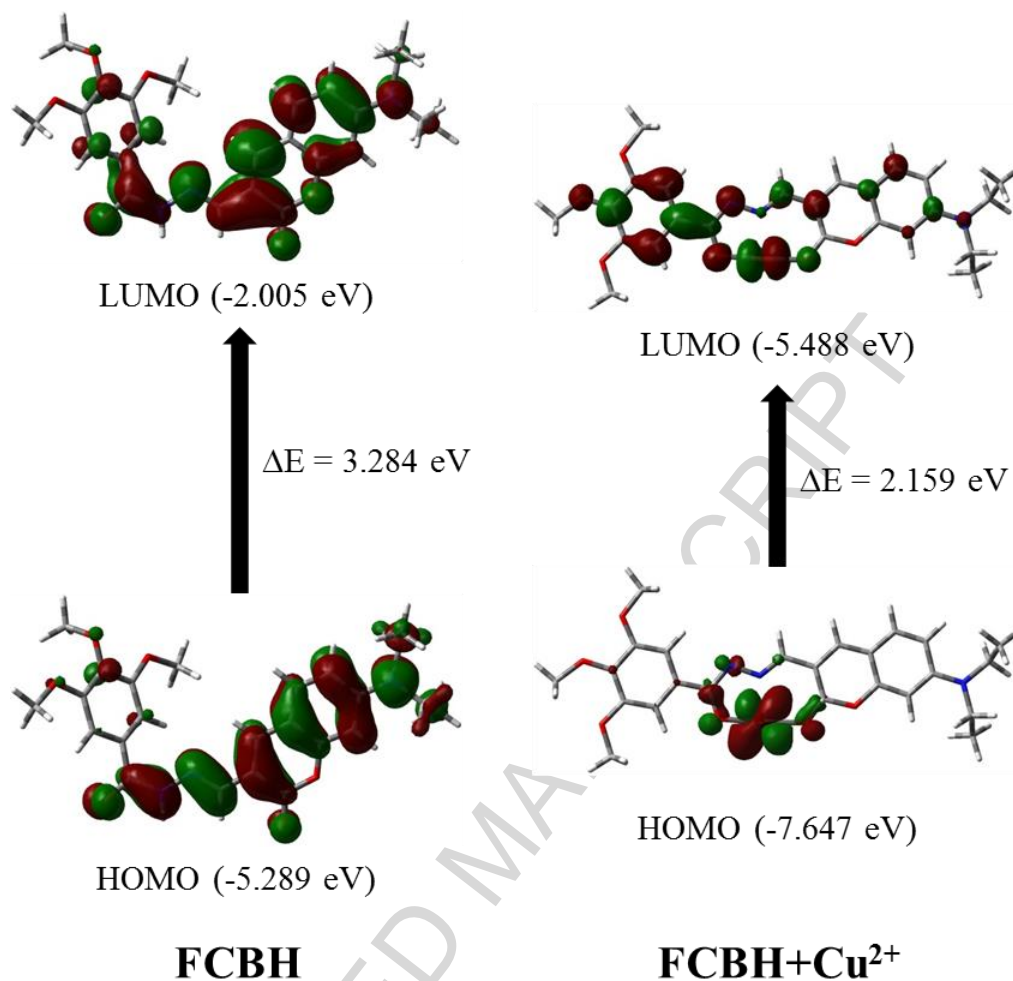


**Fig. 8.** HOMO-LUMO energy level diagram of **FCBH** and its corresponding Cu<sup>2+</sup> complex.

### 3.7. pH effect on the sensing behavior

The effects of pH on the fluorescence emission of **FCBH** in the absence and presence of Cu<sup>2+</sup> (1 equiv.) were determined (Fig. 9). For **FCBH**, an obvious increase in the peak bonded at 521 nm was observed when the pH value changed from 2 to 7. A possible reason could be that the highly protonated receptor is slowly dissociated into its free receptor. Similar spectral changes were obtained for **FCBH-Cu<sup>2+</sup>** at acidic pH conditions, indicating that the protonation of the receptor lowers its coordination ability, and a sudden decrease in emission at neutral pH is

due to the formation of the metal complex. Over the pH range of 8–10, the fluorescence quenching was observed in both cases. This can be explained by the fact that the deprotonation occurs in alkaline pH conditions, which prevents the coordination ability of the receptor towards the metal ion. The results reveal that the deprotonation process involved in the formation of the **FCBH**-Cu<sup>2+</sup> complex and the Cu<sup>2+</sup> recognition process is free from pH interference under neutral pH conditions.

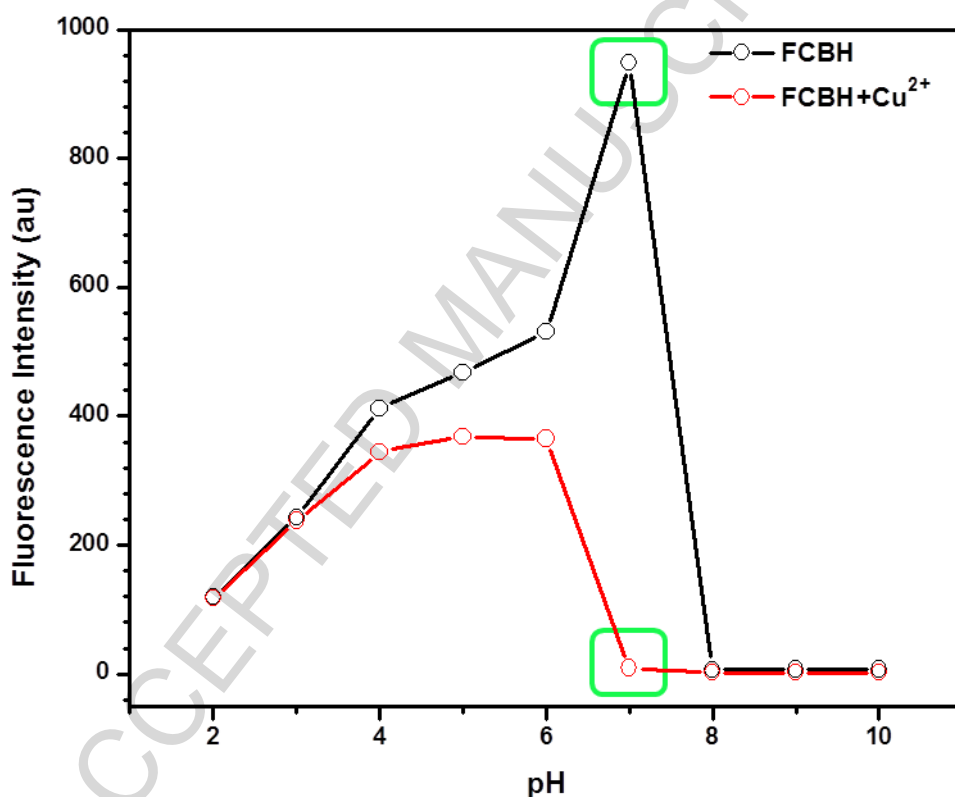


**Fig. 9.** Fluorescence intensity (at  $\lambda_{\max}$  of 521 nm) of **FCBH** and **FCBH**-Cu<sup>2+</sup> at various ranges of pH.

### 3.8. Competitive selectivity of **CS** to Al<sup>3+</sup> over other metal ions

To further estimate the selectivity of **FCBH** for  $\text{Cu}^{2+}$ , the competitive experiment in the presence of other metal ions including  $\text{Co}^{2+}$ ,  $\text{Al}^{3+}$ ,  $\text{Cr}^{3+}$ ,  $\text{Fe}^{3+}$ ,  $\text{Hg}^{2+}$ ,  $\text{Mg}^{2+}$ ,  $\text{Pb}^{2+}$ ,  $\text{Mn}^{2+}$ ,  $\text{Ni}^{2+}$  and  $\text{Zn}^{2+}$  under the same conditions was examined (Fig. 10). It is noticeable that upon addition of  $\text{Cu}^{2+}$  to **FCBH** in the presence of competitive metal ions shown immediate response in absorbance and emission. Decrease in absorbance and quenching in emission could be due to strong binding ability of copper ion and suitable coordination geometry conformation of ligand. These results reveal that the recognition of  $\text{Cu}^{2+}$  by probe **FCBH** is not significantly influenced by other competitive metal ions and it could be used as a selective chemosensor for  $\text{Cu}^{2+}$ .

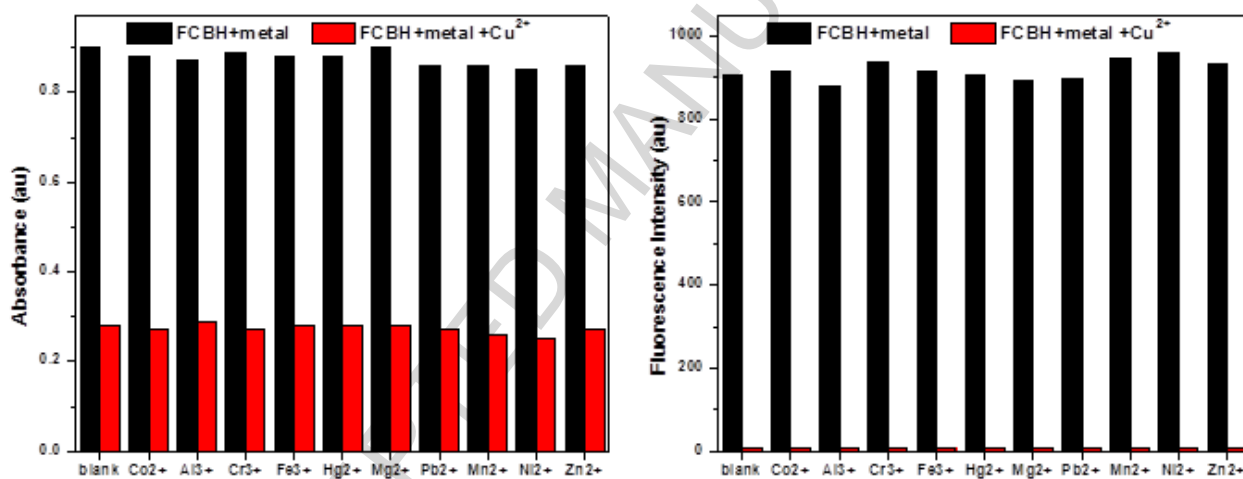


**Fig. 10.** UV-Vis absorbance (at  $\lambda_{\text{max}} = 457 \text{ nm}$ ) and fluorescence emission (at  $\lambda_{\text{max}} = 521 \text{ nm}$ ) responses of **FCBH** to  $\text{Cu}^{2+}$  in the presence of various metal ions.

### 3.8. Practical applications

**FCBH** is a favorable selective colorimetric and fluorescent chemosensor for  $\text{Cu}^{2+}$  in DMSO/water (1:1, v/v) media. To get a practical application view, electrospun nanofibers blended with **FCBH** were prepared to sense  $\text{Cu}^{2+}$  in aqueous solution. As we expected, receptor-blended ES test strips were successfully examined in water/EtOH (9:1, v/v).

The morphologies of the electrospun nanofibers were characterized by SEM analysis. The film was composed of numerous, smooth and randomly oriented cross-linked nanofibers (Fig. S2). **FCBH**-blended nanofibers exhibited similar morphology to that observed in pure polyurethane nanofibers. The SEM results showing the uniform distribution of material on the nanofibers. However an electrospun fiber from this process typically has a diameter in the range of 500-1000 nm. We obtained small nanofibers in large quantities and with a uniform size. **FCBH**-blended ES thin films were further used as test strips for the detection of  $\text{Cu}^{2+}$ .

To examine selectivity, the test strips were sprayed with solutions containing various cations, such as  $\text{Zn}^{2+}$ ,  $\text{Pb}^{2+}$ ,  $\text{Al}^{3+}$ ,  $\text{Co}^{2+}$ ,  $\text{Cr}^{3+}$ ,  $\text{Cu}^{2+}$ ,  $\text{Fe}^{3+}$ ,  $\text{Hg}^{2+}$ ,  $\text{Mg}^{2+}$ ,  $\text{Mn}^{2+}$  and  $\text{Ni}^{2+}$  (100  $\mu\text{M}$ ). As shown in Fig. 11, a significant visible color change from greenish-yellow to red was observed immediately after the addition of  $\text{Cu}^{2+}$ , and green fluorescence quenching was also observed under UV light. Furthermore, the sensing behavior of the **FCBH**-blended electrospun thin film was also investigated by confocal laser scanning microscopy (CLSM). A mixture of ethanol and water (9:1, v/v) containing  $\text{Cu}^{2+}$  (100  $\mu\text{M}$ ) was dropped onto the surface of an **FCBH**-blended nanofiber strip, and CLSM was subsequently performed using an excitation wavelength at 475 nm. The free state of the **FCBH**-blended nanofiber shows a bright yellow fluorescence (Fig. 12). The fluorescence on the surface of the nanofibers is almost completely quenched upon addition of  $\text{Cu}^{2+}$ . This experiment indicates that the sensor is quite useful for the rapid in situ detection of  $\text{Cu}^{2+}$ .

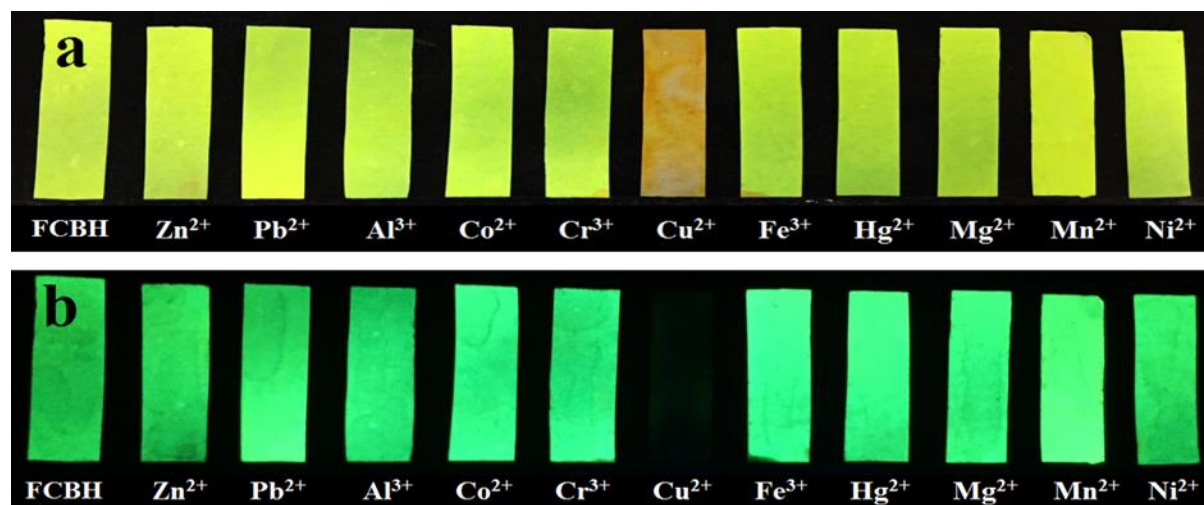


**Fig. 11.** Color change of **FCBH**-blended electrospun nanofiber test strips after treatment with various metal ions under normal (a) and UV (b) lights.

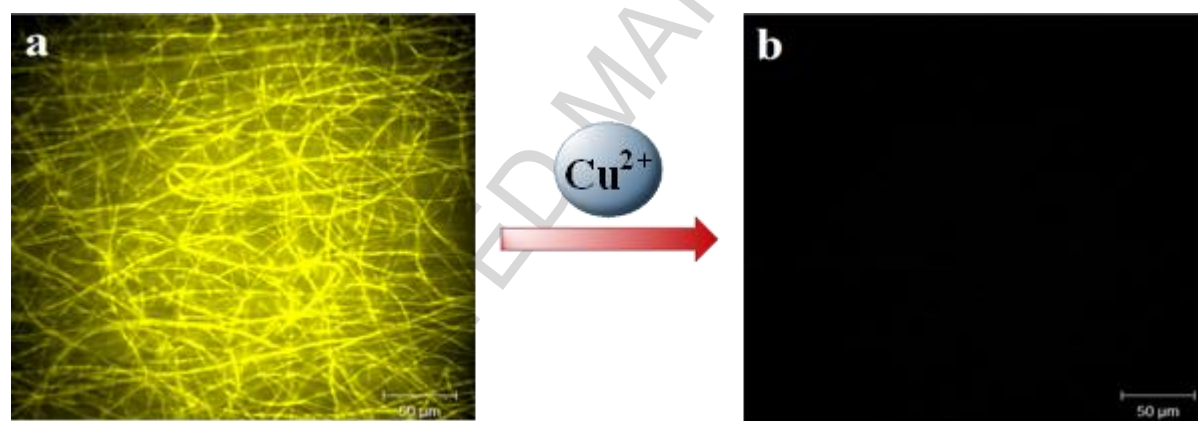


**Fig. 12.** Fluorescence confocal images of color variations of **FCBH**-blended electrospun nanofibers upon treating with  $\text{Cu}^{2+}$  ions.

### 3.9. UV-Vis and fluorescence response of the **FCBH**- $\text{Cu}^{2+}$ complex towards anions

We subsequently studied the chemical reversibility behavior of **FCBH**- $\text{Cu}^{2+}$  by absorption and fluorescence experiments in DMSO-water solution. For this purpose, **FCBH**- $\text{Cu}^{2+}$  was treated with a variety of anions such as  $\text{Cl}^-$ ,  $\text{Br}^-$ ,  $\text{I}^-$ ,  $\text{F}^-$ ,  $\text{OH}^-$ ,  $\text{CN}^-$ ,  $\text{SCN}^-$ ,  $\text{HS}^-$ ,  $\text{N}_3^-$ ,

$\text{NO}_3^-$ ,  $\text{ClO}_4^-$  and  $\text{H}_2\text{PO}_4^-$  (20  $\mu\text{M}$ ). As depicted in Fig. 13, UV-Vis spectra returned to their original state of **FCBH**, and the quenched fluorescence of the **FCBH-Cu<sup>2+</sup>** complex was restored upon addition of  $\text{CN}^-$  to the solution of **FCBH-Cu<sup>2+</sup>**. Meanwhile, the red color of the **FCBH**-blended electrospun thin film with  $\text{Cu}^{2+}$  immediately returned to the initial yellow color upon the addition of  $\text{CN}^-$  (Fig. 13, inset), resulting from the formation of more stable copper complexes such as  $[\text{Cu}(\text{CN})_4]^{3-}$  and  $[\text{Cu}(\text{CN})_2]^-$  [49]. The color of the recovered **FCBH**-blended electrospun nanofiber thin film was regenerated upon further addition of copper ions. However, other anion species caused almost no change in the absorption and fluorescence spectra under the same conditions.

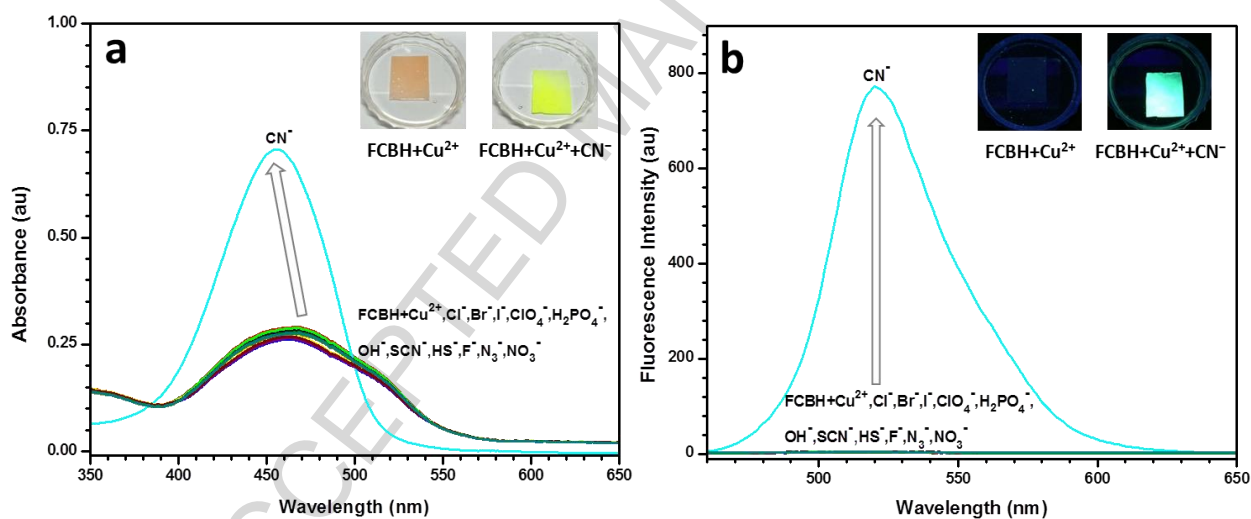


**Fig. 13.** Absorption (a) and fluorescence (b) spectra of **FCBH-Cu<sup>2+</sup>** in the presence of various anion species. Inset: Images of proof of reversibility.

The reversibility and regeneration of sensing probes are important factors in practical applications. The alternate additions of a constant level (20  $\mu\text{M}$ ) of  $\text{Cu}^{2+}$  and  $\text{CN}^-$  to the solution of **FCBH** gives rise to a switchable change in the fluorescence emission at 521 nm (Fig. 14).

This reversible fluorescence behavior of **FCBH** can be repeated several times by alternating  $\text{Cu}^{2+}/\text{CN}^-$  addition. These results demonstrate that the metal binding of **FCBH** is chemically reversible, and the **FCBH** probe can be used as a reversible colorimetric and fluorometric chemosensor for  $\text{Cu}^{2+}$  ions.

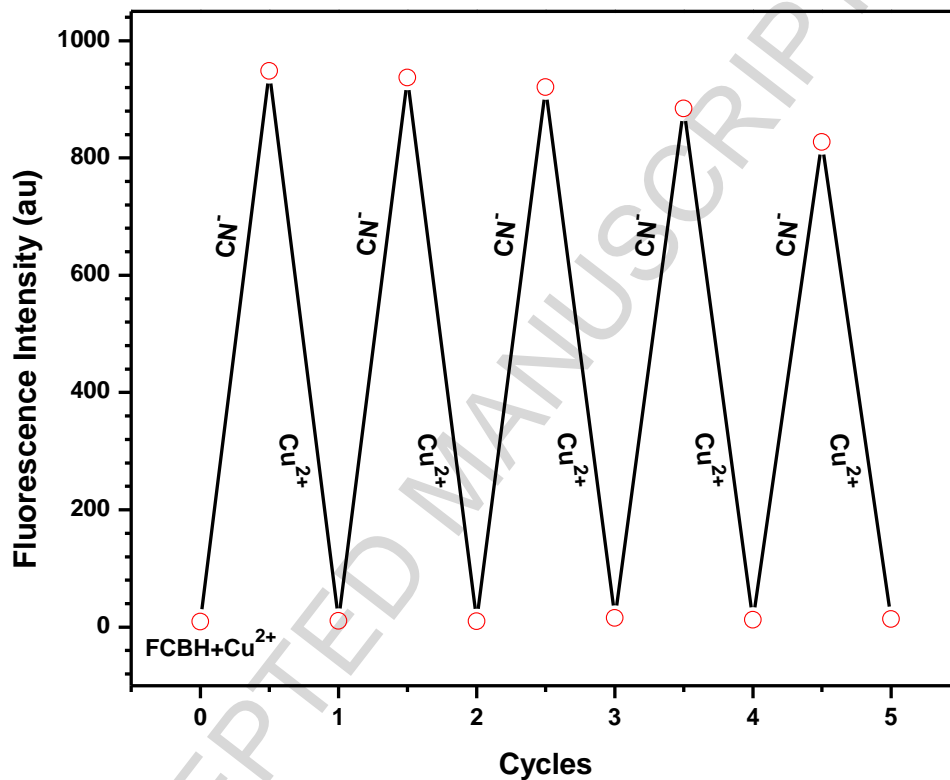


**Fig. 14.** Changes in fluorescence of **FCBH** (20  $\mu\text{M}$ ) at 521 nm upon alternate addition of a constant amount of  $\text{Cu}^{2+}$  and  $\text{CN}^-$  (1 equiv.).

From previous studies, the possible binding mode between **FCBH** and  $\text{Cu}^{2+}$  is shown in Fig. 15. The fluorescent ligand **FCBH** is a slightly twisted, non-planar, highly conjugated  $\pi$ -electron system. Upon addition of  $\text{Cu}^{2+}$ , the non-planar structure is converted into a planar

structure, and the fluorescence of the ligand is completely quenched due to the strongly bonded paramagnetic nature of  $\text{Cu}^{2+}$  ion.

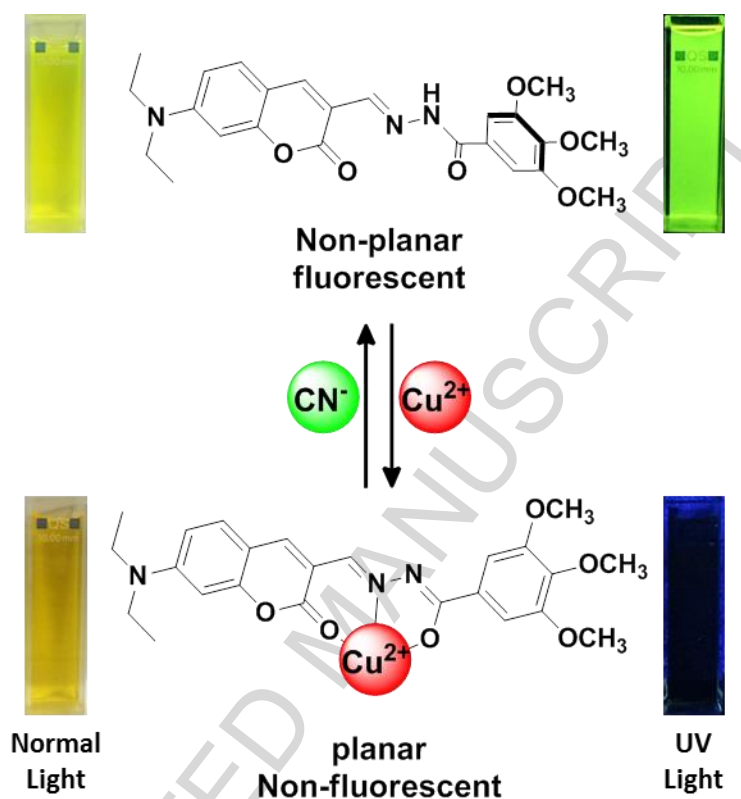


**Fig. 15.** Proposed mode of complexation between **FCBH** and  $\text{Cu}^{2+}$ . Observed naked-eye (left) and fluorescence (right) changes upon **FCBH**- $\text{Cu}^{2+}$  complexation and subsequent treatment with  $\text{CN}^-$  are shown.

#### 4. Conclusions

In conclusion, we have synthesized a new coumarin-based chemosensor (**FCBH**), which showed a reversible fluorescence quenching response toward  $\text{Cu}^{2+}$  via a 1:1 binding mode in aqueous solution. The addition of  $\text{Cu}^{2+}$  causes a visible color change from greenish-yellow to red, as well as green fluorescence quenching. Meanwhile, the **FCBH** probe displayed excellent

selectivity for  $\text{Cu}^{2+}$  over other tested metal ions. The binding mode and the corresponding quenching mechanism were examined by UV-Vis, fluorescence, ESI-MS, and  $^1\text{H}$  NMR techniques, as well as DFT calculations. The  $\text{Cu}^{2+}$ -induced fluorescence quenching can be attributed to CHEQ. Furthermore, **FCBH**-blended electrospun nanofiber test strips could selectively detect  $\text{Cu}^{2+}$  ions in aqueous solution. Further studies of the **FCBH**- $\text{Cu}^{2+}$  mixture revealed that the fluorescence quenching was reversible in the presence of  $\text{CN}^-$  ions.

### Acknowledgements

This study was supported by the National Research Foundation of Korea (NRF) funded by the Ministry of Science, ICT and Future Planning (Grant no. NRF-2014M3C1A9060739).

### References

- [1] J.S. Kim, D.T. Quang, Calixarene-derived fluorescent probes, *Chem. Rev.* 107 (2007) 3780–3799.
- [2] H.N. Kim, M.H. Lee, H.J. Kim, J.S. Kim, J. Yoon, A new trend in rhodamine-based chemosensors: Application of spiro lactam ring-opening to sensing ions, *Chem. Soc. Rev.* 37 (2008) 1465–1472.
- [3] X. Chen, T. Pradhan, F. Wang, J.S. Kim, J. Yoon, Fluorescent chemosensors based on spiro ring-opening of xanthenes and related derivatives, *Chem. Rev.* 112 (2012) 1910–1956.
- [4] M. P. Anderson, R. J. Gregory, S. Thompson, D. W. Souza, S. Paul, R. C. Mulligan, A. E. Smith, M. J. Welsh, Demonstration that CFTR is a chloride channel by alteration of its anion selectivity, *Science* 253 (1991) 202–205.

- [5] J. F. Clark, D. L. Clark, G. D. Whitener, N. C. Schroeder, S. H. Straus, Isolation of soluble  $^{99}\text{Tc}$  as a compact solid using a recyclable, redox-active, metal-complex extractant, *Environ. Sci. Technol.* 30 (1996) 3124–3127.
- [6] Y. Yamini, N. Alizadeh, M. Shamsipur, Solid phase extraction and determination of ultra trace amounts of mercury(II) using octadecyl silica membrane disks modified by hexathia-18-crown-6-tetraone and cold vapour atomic absorption spectrometry, *Anal. Chim. Acta* 355 (1997) 69–74.
- [7] C.F. Harrington, S.A. Merson, T.M.D. D’Silva, Method to reduce the memory effect of mercury in the analysis of fish tissue using inductively coupled plasma mass spectrometry, *Anal. Chim. Acta* 505 (2004) 247–254.
- [8] S.L.C. Ferreira, A.S. Queiroz, M.S. Fernandes, H.C. dos Santos, Application of factorial designs and Doehlert matrix in optimization of experimental variables associated with the preconcentration and determination of vanadium and copper in seawater by inductively coupled plasma optical emission spectrometry, *Spectrochim. Acta B* 57 (2002) 1939–1950.
- [9] J.C. Yu, J.M. Lo, K.M. Wai, Extraction of gold and mercury from sea water with bismuth diethyldithiocarbamate prior to neutron activation— $\gamma$ -spectrometry, *Anal. Chim. Acta* 154 (1983) 307–312.
- [10] A. Ali, H. Shen, X. Yin, Simultaneous determination of trace amounts of nickel, copper and mercury by liquid chromatography coupled with flow injection online derivatization and preconcentration, *Anal. Chim. Acta* 369 (1998) 215–223.
- [11] A. Bobrowski, K. Nowak, J. Zarebski, Application of a bismuth film electrode to the Voltammetric determination of trace iron using a  $\text{Fe(III)-TEA-BrO}_3^-$  catalytic system, *Anal. Bioanal. Chem.* 382 (2005) 1691–1697.

- [12] V.K. Gupta, L.P. Singh, R. Singh, N. Upadhyay, S.P. Kaur, B. Sethi, A novel copper (II) selective sensor based on Dimethyl 4, 4' (o-phenylene) bis(3-thioallophanate) in PVC matrix, *J. Mol. Liq.* 174 (2012) 11–16.
- [13] V.K. Gupta, B. Sethi, R.A. Sharma, S. Agarwal, A. Bharti, Mercury selective potentiometric sensor based on low rim functionalized thiacalix [4]-arene as a cationic receptor, *J. Mol. Liq.* 177 (2013) 114–118.
- [14] S. Karthikeyan, V.K. Gupta, R. Boopathy, A. Titus, G. Sekaran, A new approach for the degradation of high concentration of aromatic amine by heterocatalytic Fenton oxidation: Kinetic and spectroscopic studies, *J. Mol. Liq.* 173 (2012) 153–163.
- [15] V.K. Gupta, S. Kumar, R. Singh, L.P. Singh, S.K. Shoor, B. Sethi, Cadmium (II) ion sensing through p-tert-butyl calix[6]arene based potentiometric sensor, *J. Mol. Liq.* 195 (2014) 65–68.
- [16] V.K. Gupta, A.K. Singh, L.K. Kumawat, Thiazole Schiff base turn-on fluorescent chemosensor for  $Al^{3+}$  ion, *Sens. Actuators B* 195 (2014) 98–108.
- [17] V.K. Gupta, A.K. Singh, N. Mergu, Antipyrine based Schiff bases as turn-on fluorescent sensors for Al(III) ion, *Electrochim. Acta* 117 (2014) 405–412.
- [18] V.K. Gupta, N. Mergu, A.K. Singh, Fluorescent chemosensors for  $Zn^{2+}$  ions based on flavonol derivatives, *Sens. Actuators B* 202 (2014) 674–682.
- [19] N. Mergu, A.K. Singh, V.K. Gupta, Highly sensitive and selective colorimetric and off-on fluorescent reversible chemosensors for  $Al^{3+}$  based on the rhodamine fluorophore, *Sensors* 15 (2015) 9097–9111.
- [20] V.K. Gupta, N. Mergu, L.K. Kumawat, A.K. Singh, A reversible fluorescence “off-on-off” sensor for sequential detection of aluminum and acetate/fluoride ions, *Talanta* 144 (2015) 80–89.

- [21] L. Prodi, F. Bolletta, M. Montalti, N. Zaccheroni, Luminescent chemosensors for transition metal ions, *Coord. Chem. Rev.* 205 (2000) 59–83.
- [22] N. Mergu, V.K. Gupta, A novel colorimetric detection probe for copper(II) ions based on a Schiff base, *Sens. Actuators B* 210 (2015) 408–417.
- [23] L.K. Kumawat, N. Mergu, A.K. Singh, V.K. Gupta, A novel optical sensor for copper ions based on phthalocyanine tetrasulfonic acid, *Sens. Actuators B* 212 (2015) 389–394.
- [24] K.P. Carter, A.M. Young, A.E. Palmer, Fluorescent sensors for measuring metal ions in living systems, *Chem. Rev.* 114 (2014) 4564–4601.
- [25] M. C. Linder, M. H. Azam, Copper biochemistry and molecular biology, *Am. J. Clin. Nutr.* 63 (1996) 797S–811S.
- [26] L. Zeng, E.W. Miller, A. Pralle, E.Y. Isacoff, C.J. Chang, A selective turn-on fluorescent sensor for imaging copper in living cells, *J. Am. Chem. Soc.* 128 (2006) 10–11.
- [27] L.M. Gaetke, C.K. Chow, Copper toxicity, oxidative stress, and antioxidant nutrients, *Toxicology* 189 (2003) 147–163.
- [28] E. Madsen, J.D. Gitlin, Copper and iron disorders of the brain, *Annu. Rev. Neurosci.* 30 (2007) 317–337.
- [29] Y.H. Hung, A.I. Bush, R.A. Cherny, Copper in the brain and Alzheimer's disease, *J. Biol. Inorg. Chem.* 15 (2010) 61–76.
- [30] J.C. Lee, H.B. Gray, J.R. Winkler, Copper(II) binding to  $\alpha$ -synuclein, the Parkinson's protein, *J. Am. Chem. Soc.* 130 (2008) 6898–6899.
- [31] C. Vulpe, B. Levinson, S. Whitney, S. Packman, J. Gitschier, Isolation of a candidate gene for Menkes disease and evidence that it encodes a copper-transporting ATPase, *Nat. Genet.* 3 (1993) 7–13.

- [32] N. Narayanaswamy, T. Govindaraju, Aldazine-based colorimetric sensors for  $\text{Cu}^{2+}$  and  $\text{Fe}^{3+}$ , *Sens. Actuators B* 161 (2012) 304–310.
- [33] L.J. Tang, F. Li, M. Liu, R. Nandhakumar, Single sensor for two metal ions: colorimetric recognition of  $\text{Cu}^{2+}$  and fluorescent recognition of  $\text{Hg}^{2+}$ , *Spectrochim. Acta A* 78 (2011) 1168–1172.
- [34] V.K. Gupta, N. Mergu, L.K. Kumawat, A new multifunctional rhodamine-derived probe for colorimetric sensing of  $\text{Cu(II)}$  and  $\text{Al(III)}$  and fluorometric sensing of  $\text{Fe(III)}$  in aqueous media, *Sens. Actuators B* 223 (2016) 101–113.
- [35] H. S. Jung, P. S. Kwon, J. W. Lee, J. I. Kim, C. S. Hong, J. W. Kim, S. Yan, J. Y. Lee, J. H. Lee, T. Joo, J. S. Kim, Coumarin-Derived  $\text{Cu}^{2+}$ -Selective Fluorescence Sensor: Synthesis, Mechanisms, and Applications in Living Cells, *J. Am. Chem. Soc.* 131 (2009) 2008–2012.
- [36] J. Xie, M. Menand, S. Maisonneuve, R. Metivier, Synthesis of Bispyrenyl Sugar-Aza-Crown Ethers as New Fluorescent Molecular Sensors for  $\text{Cu(II)}$ , *J. Org. Chem.* 72 (2007) 5980–5985.
- [37] L. Huang, J. Cheng, K. Xie, P. Xi, F. Hou, Z. Li, G. Xie, Y. Shi, H. Liu, D. Bai, Z. Zeng,  $\text{Cu}^{2+}$ -selective fluorescent chemosensor based on coumarin and its application in bioimaging, *Dalton Trans.* 40 (2011) 10815–10817.
- [38] J.-T. Yeh, W.-C. Chen, S.-R. Liu, S.-P. Wu, A coumarin-based sensitive and selective fluorescent sensor for copper(II) ions, *New J. Chem.* 38 (2014) 4434–4439.
- [39] V.K. Gupta, N. Mergu, L.K. Kumawat, A.K. Singh, Selective naked-eye detection of magnesium (II) ions using a coumarin-derived fluorescent probe, *Sens. Actuators B* 207 (2015) 216–223.

- [40] O. Garcia-Beltran, B.K. Cassels, C. Perez, N. Mena, M.T. Nunez, N.P. Martinez, P. Pavez, M.E. Aliaga, Coumarin-based fluorescent probes for dual recognition of copper(II) and iron(III) ions and their application in bio-imaging, *Sensors* 10 (2014) 1358–1371.
- [41] M.J. Frisch, G.W. Trucks, H.B. Schlegel, G.E. Scuseria, M.A. Robb, J.R. Cheeseman, G. Scalmani, V. Barone, B. Mennucci, G.A. Petersson, et al., *Gaussian 09, Revision E.01*, Gaussian Inc., Wallingford, CT, 2013.
- [42] Y. Zhao, D.G. Truhlar, The M06 suite of density functionals for main group thermochemistry, thermochemical kinetics, noncovalent interactions, excited states, and transition elements: Two new functionals and systematic testing of four M06-class functionals and 12 other functionals. *Theor. Chem. Acc.* 120 (2008) 215–241.
- [43] W. Xuan, C. Chen, Y. Cao, W. He, W. Jiang, K. Liu, W. Wang, Rational design of a ratiometric fluorescent probe with a large emission shift for the facile detection of  $\text{Hg}^{2+}$ , *Chem. Commun.* 48 (2012) 7292–7294.
- [44] C. Kim, J.-Y. Hwang, K.-S. Ku, S. Angupillai, Y.-A. Son, A renovation of non-aqueous  $\text{Al}^{3+}$  sensor to aqueous media sensor by simple recyclable immobilize electrospun nano-fibers and its uses for live sample analysis, *Sens. Actuators B* 228 (2016) 259–269.
- [45] D. Jimenez, R. Martinez-Manez, F. Sancenon, J. Soto, Electro-optical triple-channel sensing of metal cations via multiple signalling patterns, *Tetrahedron Lett.* 45 (2004) 1257–1259.
- [46] S.A. Lee, G.R. You, Y.W. Choi, H.Y. Jo, A.R. Kim, I. Noh, S.-J. Kim, Y. Kim, C. Kim, A new multifunctional Schiff base as a fluorescence sensor for  $\text{Al}^{3+}$  and a colorimetric sensor for  $\text{CN}^-$  in aqueous media: An application to bioimaging, *Dalton Trans.* 43 (2014) 6650–6659.

- [47] J.H. Chang, Y.M. Choi, Y.-K. Shin, A significant fluorescence quenching of anthrylaminobenzocrown ethers by paramagnetic metal cations, *Bull. Korean Chem. Soc.* 22 (2001) 527–530.
- [48] J.-T. Yeh, W.-C. Chen, S.-R. Liu, S.-P. Wu, A coumarin-based sensitive and selective fluorescent sensor for copper(II) ions, *New J. Chem.* 38 (2014) 4434–4439.
- [49] R. Parkash, J. Zyka, The reaction between copper(II) and cyanide ions, *Microchem. J.* 17 (1972) 309–317.

ACCEPTED MANUSCRIPT



## Highlights

- Coumarin-based receptor bearing the benzohydrazide was developed as a fluorescent chemosensor.
- It has been applied for the monitoring of copper ions in aqueous solution.
- A good naked-eye color change from greenish yellow (fluorescence-ON) to red (fluorescence-OFF) was observed with  $\text{Cu}^{2+}$  ion.
- The quenched fluorescence of  $\text{Cu}^{2+}$  complex was restored upon addition of  $\text{CN}^-$  ions.
- Electrospun nanofiber test strips were prepared for the detection of  $\text{Cu}^{2+}$  ions in aqueous medium.